Title
Some Aspects of the Relativistic Many-Body Theory of Baryonic Systems

Authors
Weber, F.
Weigel, M.K.

Publication Date
1990-04-01

LBL-28922
Preprint

Lawrence Berkeley Laboratory
UNIVERSITY OF CALIFORNIA

Submitted to Nuclear Physics A

Some Aspects of the Relativistic Many-Body Theory of Baryonic Systems

F. Weber and M.K. Weigel

April 1990

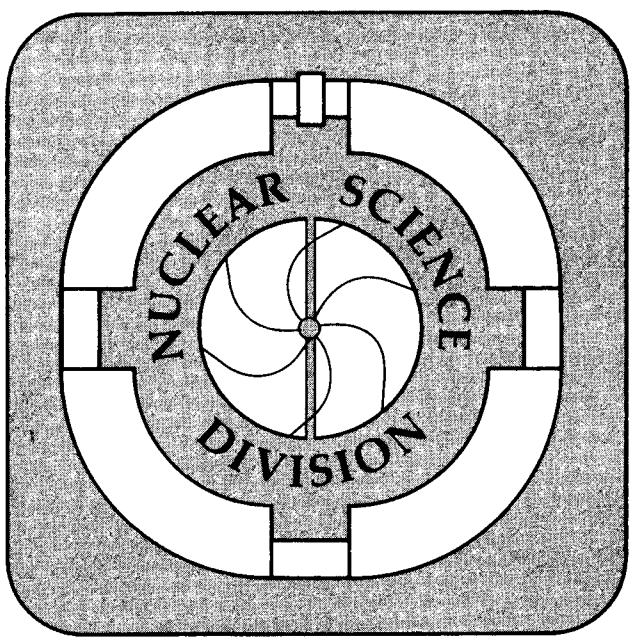

Prepared for the U.S. Department of Energy under Contract Number DE-AC03-76SF00098.

DISCLAIMER

LBL - 28922

Some Aspects of the Relativistic Many-Body Theory of Baryonic Systems*

F. Weber† and M. K. Weigel,‡

Nuclear Science Division
Lawrence Berkeley Laboratory
University of California
Berkeley, California 94720, U.S.A.

PACS numbers: 11.10.Ef, 21.30., 21.65.+f, 97.60.Jd

* This work was supported by the Director, Office of Energy Research, Office of High Energy and Nuclear Physics, Division of Nuclear Physics, of the U. S. Department of Energy under Contract DE-AC03-76SF00098 and the Max Kade Foundation of New York.

† Max Kade Foundation Research Fellow. Permanent address: Institute for Theoretical Physics, University of Munich, Theresienstrasse 37/III, D-8000 Munich 2, Federal Republic of Germany.

‡ Sektion Physik of the University of Munich, Am Coulombwall 1, D-8046 Garching, Federal Republic of Germany.

Abstract

Some basic features of the relativistic treatment of many-body systems (nuclear matter, neutron matter, electrically charge neutral many-baryon/lepton neutron star matter) are discussed and illustrated by some selected examples. After a short review of the Hartree and Hartree-Fock approximation, special attention is given to the basic structure of Brueckner-type approaches.

I. Introduction

In the last decade there has been rising interest in describing nuclear systems, like nuclear matter, neutron matter, and neutron star matter, in a relativistic many-body quantum field approach. (More details are given in refs. 1 and 2.) Relativistic methods are advantageous in several respects; among these are, for instance:[1,2] The shift of the equilibrium density of nuclear matter from the so-called Coester line towards the equilibrium density of nuclear matter ($\varrho_0 \approx 0.15$ fm^{-3}) via a new saturation mechanism; the relativistic analysis of scattering data; the description of finite systems and the natural incorporation of the spin-orbit force. Of great importance is also the access to the equation of state (EOS) of high-density matter, encountered in the treatment of astrophysical problems and the analysis of heavy-ion reactions. Naturally, there exists a great interest to explore the quantum field approach in many respects in a more microscopic framework. To mention are, for example, the consideration of consistency questions, predictive power and limitations of the method, etc.

II. General considerations

In a rather rough scheme one can illustrate the attempt of treating the relativistic nuclear many-body problem as given in table 1, where the types of different dynamical descriptions (i.e. Lagrangians) versus many-body approximations are sketched. More or less explored are the parts labeled by crosses, where - due to its simplicity - the Hartree (H) approximation has been utilized in most cases. We have concentrated ourselves on the parts denoted by circles. Of course, table 1 oversimplifies since one can add other features like, for instance: renormalization, random phase approximation, finite temperature effects, etc.[1] In the given scheme, the Hartree and Hartree-Fock (HF) approximations belong to the phenomenological theories (i.e., no saturation with "free" one-boson-exchange po-

tential parameters).[2,3] In the framework of these approaches one has to adjust the coupling strenghts to "basic nuclear parameters", i.e. binding energy, effective mass, incompressibility, symmetry energy at saturation density ϱ_0 of normal nuclear matter, which themselves are not accurately known. For instance, the incompressibility K is expected to lie in the range between 200 and 350 MeV; for the effective mass m^* one has the bandwidth 0.6 - 0.85 m_N (m_N denotes the nucleon mass).[4] The general benefit of both the Hartree as well as the Hartree-Fock approximation is their capacity to describe nuclear properties near saturation satisfactorily. However in the Hartree scheme one needs σ meson self-interactions.[1] The Hartree-Fock approximation can get along ($K \approx 300$ MeV, $m^* \approx 0.7\, m_N$) without σ self-interactions by selecting more sophisticated Lagrangians (i.e., σ, ω, π and ϱ mesons).[5] Common to both of these models is their great flexibility to fit the saturation region of nuclear matter with different coupling constants, which reduce their predictive power for the high-density extrapolation.[4,5] The latter is of interest for high-energy heavy-ion reactions and astrophysical questions (e.g. neutron stars).[6] This flexibility (and resulting uncertainty) is illustrated in figs. 1 and 2, where we exhibit the different (theoretical) baryon/lepton compositions of a neutron star in the Hartree and Hartree-Fock approximation, respectively.[6] In fig. 3 we show firstly the relativistic saturation mechanism (with higher densities one has a decrease of the (σ meson) attraction (m^* decreases) and an increase of the (ω meson) repulsion, which together acts as a density-dependent interaction becoming more repulsive at higher densities; free spinors lead to the old saturation mechanism (see also fig. 6)) in the Hartree-Fock theory and secondly the different behavior of the "kinetic" (i.e. Dirac) and potential part of the energy for two Lagrangians, which both lead to the same density and energy at saturation (K differs!). Figure 4 exhibits the dependence of the EOS on m^* and K; near saturation the equation of state is determined by K, but for higher densities the behavior is solely determined by m^*. Due to the described uncertainties of the

phenomenological approach, one may be tempted to resort back to more sophisticated many-body theories, which can get along with the use of one-boson-exchange potentials.

III. Theory

A useful tool for the description of many-body systems is the Green's function scheme.[1-3] Here one has to solve - for Brueckner-type approximations - the coupled system of the Dyson equation for the two-point Greens function (denoted by G) and the effective scattering matrix T in matter (G^0 is the free two-point function):[1-3]

$$\left([G^0(1,2)]^{-1} \; - \; \Sigma(1,2) \right) \; G(2,1') \; = \; \delta(1,1') \, , \tag{1}$$

$$\begin{aligned} < 1\,2|T|1'\,2' > = \; & < 1\,2|v|1'\,2' \; - \; 2'\,1' > \\ & + \; i \; < 1\,2|v|3\,4 > \; \Lambda(34,56) \; < 5\,6|T|1'\,2' > \, , \end{aligned} \tag{2}$$

respectively, where the self-energy Σ given by

$$\Sigma(1,2) \; = \; -i \; < 1\,4|T|5\,2 > \; G(5,4) \, . \tag{3}$$

The Hartree and Hartree-Fock approximations result from eqs. (1)-(3) by setting $T = v$ and $T = v - v^{ex}$, respectively. The quantity v stands for the nucleon-nucleon interaction in free space as described, for example, by the Ho2 and HEA meson-exchange models for the nucleon-nucleon interaction. In the case of the T matrix formalism one can choose for the intermediate particle-particle propagator either the Brueckner propagator,[1,2] or the propagators of the so-called Λ treatment. These are given by[3] $\Lambda^{00} \equiv iG^0G^0$, $\Lambda^{10} \equiv \frac{i}{2}(GG^0 + G^0G)_{\rm sym}$, and $\Lambda^{11} \equiv iGG$ and correspond to the so-called Λ^{00}, Λ^{10}, and Λ^{11} approximations,

respectively. A useful simplification can be achieved by utilizing the spectral representation of the two-point Green's function, i.e.

$$G(p) = \int_{-\infty}^{+\infty} d\omega \, \frac{A(\omega, \vec{p})}{\omega - (p^0 - \mu)\,(1 + i\eta)} \,, \tag{4}$$

since all desired quantities can be expressed in terms of the self-energy Σ and the spectral function A alone.[3,6] In comparison with the non-relativistic case, the problem is much more complicated since one needs for the solution a *self − consistent* particle (anti-particle) basis. The use of *free* spinors gives essentially the old saturation mechanism with its drawbacks. A further complication is the atypical structure - in comparison with the non-relativistic case - of the relativistic spectral function. Due to the Dirac character of the baryons, one has to deal simultaneously with three (i.e., scalar, vector, and time-like) spectral functions. For instance, the scalar spectral function, A_S, takes the form ($\Sigma_i \equiv \Lambda_i + i\Gamma_i$ with $i = S, V, 0$;[3,8] $\omega_{1,2}(\vec{p}) = \Sigma_0 \pm [(m_N + \Sigma_S)^2 + (|\vec{p}| + \Sigma_V)^2]^{1/2}$ is the energy-momentum relation of particles (1) and anti-particles (2), respectively):

$$\begin{aligned}
&A_S(p^0 - \mu, \vec{p}) = \\
&= \frac{1}{\pi}\Big[\big[[m_N + \Lambda_S(p)]^2 + [|\vec{p}| + \Lambda_V(p)]^2 - [\Lambda_0(p) - p_0]^2 \\
&- \Gamma_S^2(p) - \Gamma_V^2(p) + \Gamma_0^2(p)\big]^2 + \Gamma^2(p)\Big]^{-1} \qquad (5a) \\
&\times \Big\{|\Gamma(p)|\ \mathrm{sign}((\mu - p^0)\Gamma(p)) \cdot [m_N + \Lambda_S(p)] - |\Gamma_S(p)|\ \mathrm{sign}((\mu - p^0)\Gamma_S(p)) \\
&\times \big[[m_N + \Lambda_s(p)]^2 + [|\vec{p}| + \Lambda_V(p)]^2 - [\Lambda_0(p) - p_0]^2 - \Gamma_S^2(p) - \Gamma_V^2(p) - \Gamma_0^2(p)\big]\Big\} \,,
\end{aligned}$$

$$\begin{aligned}
&\overset{\Gamma_i \to 0}{\longrightarrow} [m_N + \Sigma_S(\omega_1, \vec{p})] \\
&\quad \times \Big|2\big[(m_N + \Sigma_S)\frac{\partial \Sigma_S}{\partial \omega_1} + (|\vec{p}| + \Sigma_V)\frac{\partial \Sigma_V}{\partial \omega_1} + (\Sigma_0 - \omega_1)\,(1 - \frac{\partial \Sigma_0}{\partial \omega_1})\big]\Big|^{-1} \\
&\quad \times \delta(p^0 - \omega_1) \;\; - \;\; (1 \to 2) \qquad (5b)
\end{aligned}$$

with

$$\Gamma(p) = 2\big\{\Gamma_S(p)[m_N + \Lambda_S(p)] + \Gamma_V(p)[|\vec{p}| + \Lambda_V(p)] \qquad (6a)$$

$$+ [\eta \, \mathrm{sign}(p^0 - \mu) - \Gamma_0(p)] \, [\Lambda_0(p) - p^0]\}$$

$$\stackrel{\Gamma_i \to 0}{\longrightarrow} 2\eta \, \mathrm{sign}(p^0 - \mu) \cdot [\Lambda_0(p) - p^0] \, . \qquad (6b)$$

It should be noted that A_S of eq. (5a) (and also A_V and A_0) consists in general of two parts,[8] of which only the first one (the δ function term of eq. (5b) obtained for $\Gamma_i \to 0$) resembles to the non-relativistic case. Presently, one has to assume $\Gamma_i = 0$.[3] With this assumption - the validity depends on the chosen many-body approximation (Λ^{00}, Λ^{10}, Λ^{11}) as well as on the covered energy range - one can solve the problem keeping full self-consistency (no effective mass approximation; the relativistic Brueckner-Hartree-Fock approximation emerges as a by-product). For $|\partial\Sigma_i/\partial p^0| < 1/2$ it is then possible to keep the particle/anti-particle distinction with energy-momentum relations ω_1 and ω_2, respectively, from above (i.e. δ-function type spectral functions; the spectral function A depends on Σ and furthermore on its energy-derivatives). Numerically it is rather difficult to solve the coupled set of equations of the Λ method (cf. eqs. (1)-(3)) by means of a self-consistent iteration procedure far from saturation.[3]

IV. Illustrative examples

In fig. 5 we show the energy per particle in nuclear matter for different Brueckner-type calculations, which clearly indicate that the nuclear density is located in relativistic calculations in the right density range. In a non-relativistic calculation, for instance for the HEA potantial,[10] one obtains for the binding energy per particle in nuclear matter the values given in table 2. It can be seen that the use of the vacuum basis (i.e., free spinors) brings an improvement, but the saturation mechanism resembles still the non-relativistic case as illustrated in fig. 6. The next two figs. 7 and 8 exhibit the behavior of the self-energy matrix elements in the self-consistent basis (the matrix elements for the anti-particle states ($\approx 600 - 700$ MeV) are almost constant for $p < p_F$ (p_F is the Fermi-momentum)

and are not given). The energy dependence of Σ is rather weak ($0 \leq p \leq p_F$), but stronger (one order of magnitude) as in the Hartree-Fock approximation.[7] The energy derivatives of Σ, which measure this dependence and enter in the spectral functions (cf. eqs. (5) and (6)), are given in fig. 9. They cause a change in the momentum distribution $\varrho(|\vec{p}\,|; p_F)$ as shown in fig. 10. In the final fig. 11 we show a nice application of the neutron star matter (electrically charge neutral many-baryon/lepton system) equation of state[6] to rotating neutron stars, treated in the framework of general relativity.[11] Shown are the rotating as well as non-rotating neutron star masses M as a function of central energy density ϵ_c. The Keplerian velocity is given in the case of the rotating star models HV and $\Lambda^{00}_{Bonn} + HV$ (see figure caption 11).

Acknowledgment

One of us (F. W.) thanks the President of the Max Kade Foundation of New York for a grant.

This work was supported by the Director, Office of Energy Research, Office of High Energy and Nuclear Physics, Division of Nuclear Physics, of the U. S. Department of Energy under Contract DE-AC03-76SF00098 and by the Max Kade Foundation of New York.

References

1) B. D. Serot and J. D. Walecka, Adv. Nucl. Phys. 16 (1986) 1, and references contained therein.

2) L. S. Celenza and C. M. Shakin, Relativistic Nuclear Physics, World Scientific Lecture Notes in Physics, Vol. 2, World Scientific (Singapore 1986), and references contained therein.

3) P. Poschenrieder and M. K. Weigel, Phys. Rev. *C*38 (1988) 471, and references contained therein.

4) J. Ramschütz, F. Weber, and M. K. Weigel,,J. of Phys. *G* (in press).

5) M. Jetter, F. Weber, and M. K. Weigel, Adjustment of the effective Lagrangian in the relativistic Hartree-Fock theory, preprint LMU 1990 (submitted to Phys. Lett. *B*).

6) F. Weber and M. K. Weigel, Nucl. Phys. *A*505 (1989) 779.

7) J. Götz, Berechnung des effektiven Einteilchenpotentials in der Hartree-Fock Näherung im Rahmen der QHD; Diplomarbeit LMU München, 1988; J. Götz et al., Phys. Lett. *B*226 (1989) 213.

8) F. Weber and M. K. Weigel, Deviations from the Single-Particle Propagation in Relativistic Many-Baryon systems, preprint LMU 1989 (submitted for publication).

9) K. Holinde, Phys. Rep. 68 (1981) 2.

10) K. Holinde, K. Erkelenz, and R. Alzetta, Nucl. Phys. *A*194 (1972) 161; *A*198 (1972) 578.

11) F. Weber, N. K. Glendenning, and M. K. Weigel, Structure and Stability of Rotating Relativistic Neutron Stars, LBL preprint 28845, 1990 (submitted to Astrophys. J.).

Figure captions

Fig. 1. Lepton/baryon composition of a neutron star in the relativistic Hartree approximation[6] as a function of nuclear density ϱ ($M/M_\odot = 1.98$ and $R = 11.16$ km at the mass peak). All charged baryon states with masses $m_B \leq 1232$ MeV (i.e., Δ particle) are taken into account. The outer surface of the star in the mass density region 7.8 (density of ^{56}Fe)$< \hat{\mu}/(\mathrm{g/cm^3}) < 10^{11}$ is taken into account by the EOS of Harrison and Wheeler; for the inner surface region, $10^{11} < \hat{\mu} < 10^{13}$ g/cm^3, the EOS of Negele and Vautherin is used.[6]

Fig. 2. Same as fig. 1, but calculated for the relativistic Hartree-Fock approximation ($M/M_\odot = 2.38$ and $R = 11.51$ km at the mass peak).[6]

Fig. 3. Illustration of the relativistic saturation mechanism in nuclear matter in the Hartree-Fock approximation, which shows the non-monotonic behavior of the "kinetic" (Dirac) and potential energy E_{kin} and E_{pot}, respectively, as a function of the Fermi-momentum p_F. The different curves belong to Lagrangians with different couplings, but the same energy per particle and density (K differs), which illustrate the flexibility of the HF approach.[7]

Fig. 4. Dependence of the EOS, i.e. energy per nucleon E/N vs. nuclear density ϱ, on the incompressibility K and the effective mass m^* ($x \equiv m^*/m_N$) in the Hartree approximation for nuclear matter. Dashed curves: $m^* = 0.85\, m_N$; solid curves: $m^* = 0.6\, m_N$. The upper lying curves correspond to K=300 MeV, the lower ones to K=240 MeV.

Fig. 5. Nuclear matter energy per particle vs. Fermi-momentum for different Brueckner-type approximations (Ho2 one-boson-exchange potential). Solid line: Λ^{00} approximation; dashed line: Λ^{10} approximation; dash-dotted line: relativistic Brueckner-Hartree-Fock approximation.

Fig. 6. Kinetic (Dirac) and potential energy of nuclear matter vs. Fermi-momentum for the relativistic Brueckner-Hartree-Fock approximation (Ho2 potential). The dashed curves correspond to the use of the self-consistent basis (i.e. non-

monotonic behavior); the solid curves give the outcome utilizing free spinors (i.e. similar to the non-relativistic saturation mechanism).

Fig. 7. Self-energy matrix element $\Sigma_{\phi\phi}$ vs. $|\vec{p}|/p_F$ calculated for the Λ^{10} approximation (HEA potential;[3,10] ϕ denotes the self-consistent *particle* states).

Fig. 8. Self-energy matrix element $\Sigma_{\phi\theta}$ vs. $|\vec{p}|/p_F$ calculated for the Λ^{10} approximation (HEA potential;[3,10] θ denotes the $anti-particle$ states).

Fig. 9. Energy derivatives $\frac{\partial\Sigma_S}{\partial p^0}$ (solid line) and $|\frac{\partial\Sigma_0}{\partial p^0}|$ (dashed line) vs. $|\vec{p}|/p_F$ in the Λ^{00} approximation (Ho2 potential [9]).

Fig. 10. Momentum distribution $\varrho(|\vec{p}|/p_F; p_F)$ vs. $|\vec{p}|/p_F$ and p_F in the Λ^{00} approximation (Ho2 potential[9]).

Fig. 11. Gravitational star mass M (in units of the solar mass $M_\odot$) vs. central energy density ϵ_c for two star models (HV and $\Lambda^{00}_{Bonn} + HV$; the latter contains the influence of two-particle correlations on the HV [6] equation of state).[11] The upper lying curves refer to stars rotating at their maximum Kepler velocities (the numbers attached to these curves give the rotational frequency in units of $\sec^{-1}$), the lower curves belong to non-rotating star models.[11]

Table 1. Illustration of different many-body approximations versus Lagrangian descriptions (Φ^4 denotes the inclusion of cubic and quartic self-interaction terms of the σ meson field).

Lagrangian (Dynamics)	H	HF	2-body correlations
		nucleons	
σ, ω	+	$\oplus$	
σ, ω, Φ^4	+	$\oplus$	
$\sigma, \omega, \pi, \varrho$	+	$\oplus$	
$\sigma, \omega, \pi, \varrho, \Phi^4$	+	$\oplus$	
$\sigma, \omega, \pi, \varrho, \eta, \delta, \phi$	+	$\oplus$	$\oplus$
		more baryons $(\Delta, \Sigma, \Lambda, \Xi, ...)$	
σ, ω, Φ^4	$\oplus$	$\oplus$	
$\sigma, \omega, \pi, \varrho, \Phi^4$	$\oplus$	$\oplus$	
$\sigma, \omega, \pi, \varrho, \eta, \delta, \phi$	$\oplus$	$\oplus$	$+ \quad (N + \Delta)$

Table 2. Binding energy at saturation density calculated for the Λ^{00} approximation using the HEA meson-exchange potential (nr=non-relativistic, sc=self-consistent).

	E/N [MeV]	ϱ [fm^{-3}]
Λ^{00} (nr)	-14.47	0.229
Λ^{60} (free spinors)	-5.72	0.127
Λ^{00} (sc basis)	-8.70	0.131

Postal Addresses

Fridolin Weber, Lawrence Berkeley Laboratory, Nuclear Science Division, University of California, 1 Cyclotron Road, Berkeley, California 94720, U.S.A.; permanent address: Institute for Theoretical Physics, Ludwig-Maximilians University of Munich, Theresienstrasse 37/III, D-8000 Munich 2, F.R.G.

Manfred K. Weigel, Sektion Physik of the Ludwig-Maximilians University of Munich, Am Coulombwall 1, D-8046 Garching, F.R.G.

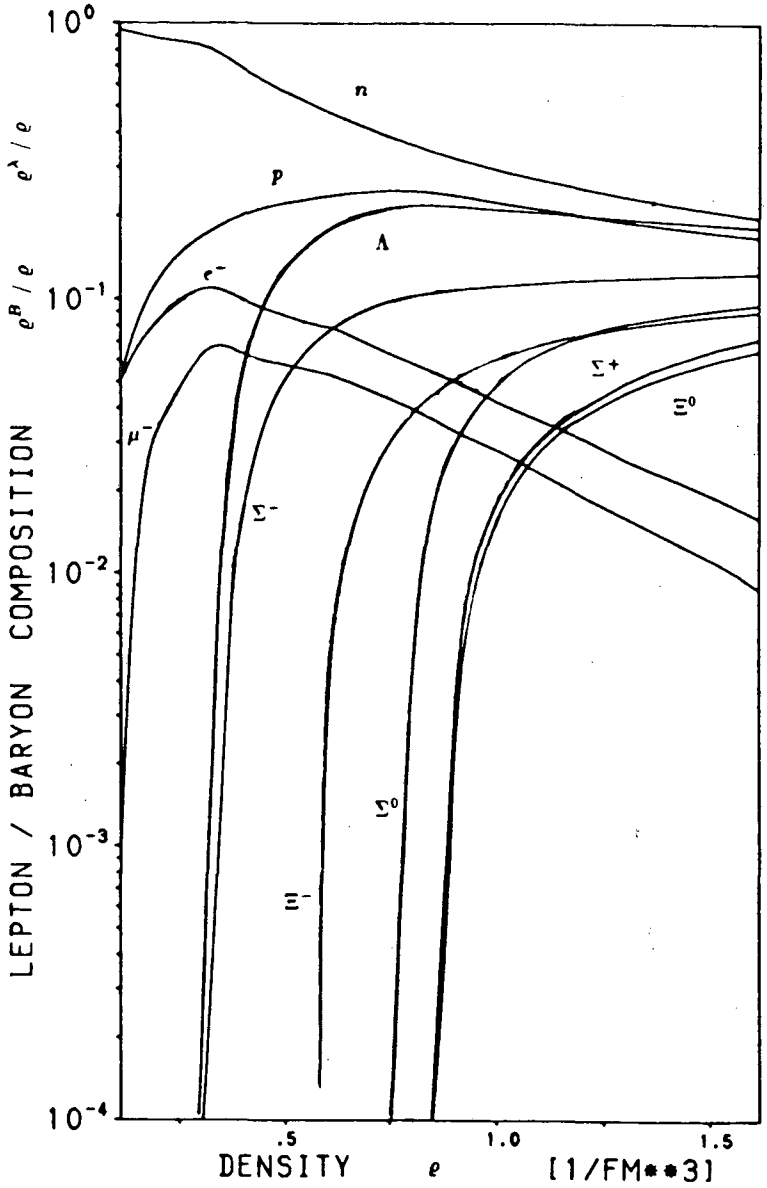
LEPTON / BARYON COMPOSITION
10^0
10^{-1}
10^{-2}
10^{-3}
10^{-4}
e^B/e
e^λ/e
n
p
Λ
e^-
μ^-
Σ^-
Ξ^-
Σ^0
Σ^+
Ξ^0
.5
1.0
1.5
DENSITY e [1/FM**3]

Fig. 1

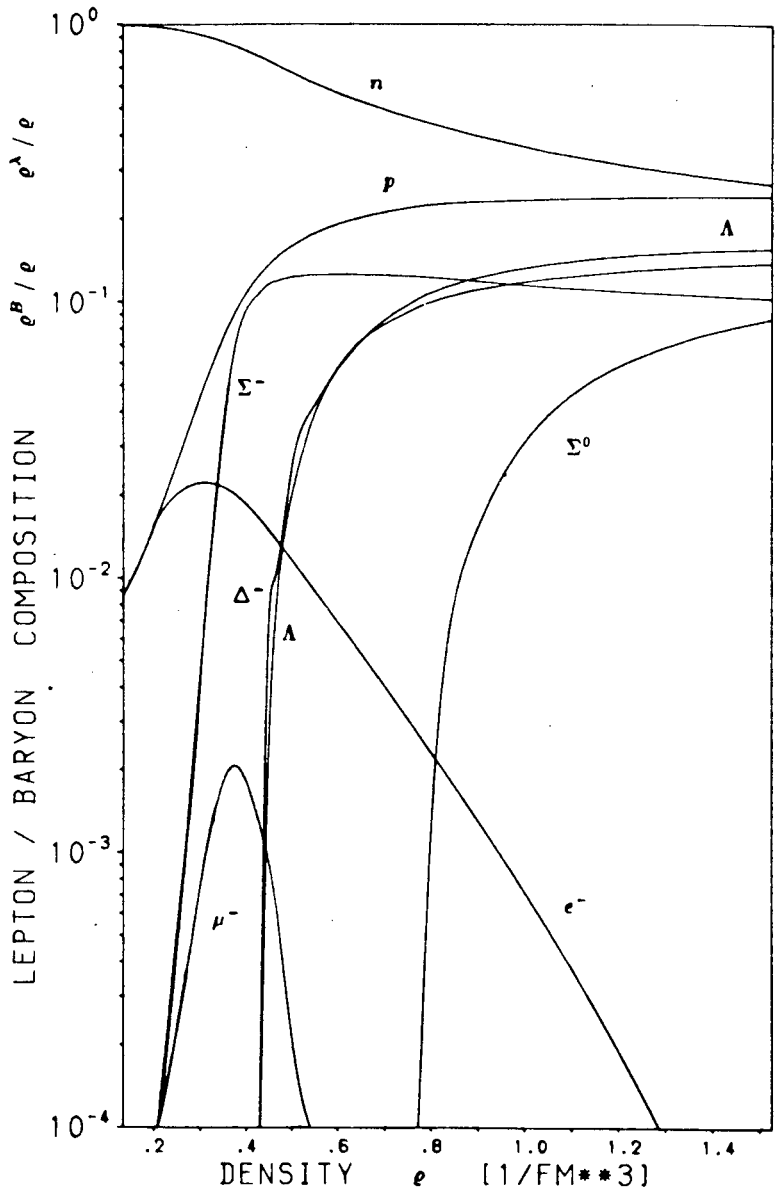
LEPTON / BARYON COMPOSITION
10^0
10^{-1}
10^{-2}
10^{-3}
10^{-4}
ϱ^B/ϱ
ϱ^λ/ϱ
n
p
Λ
Σ⁻
Σ⁰
Δ⁻
Λ
μ⁻
e⁻
.2
.4
.6
.8
1.0
1.2
1.4
DENSITY ϱ [1/FM**3]

Fig. 2

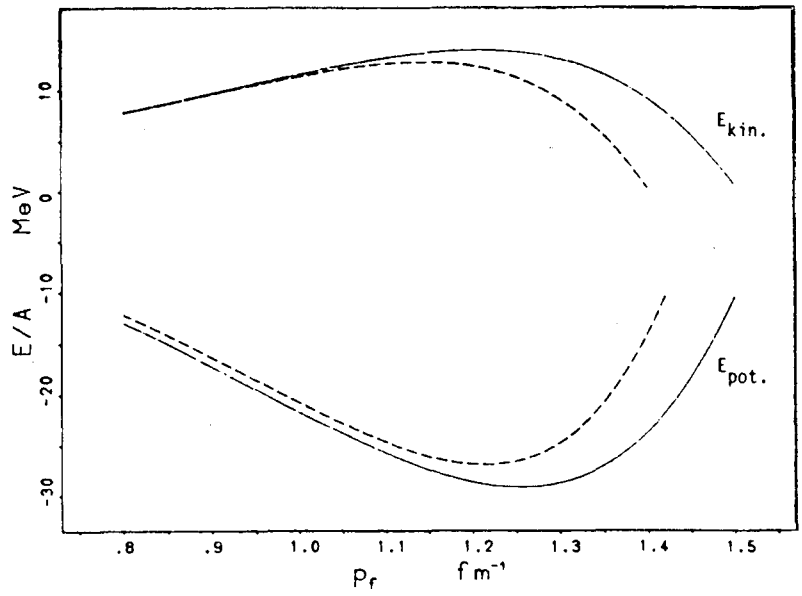
E/A MeV
10
0
-10
-20
-30
$E_{kin.}$
$E_{pot.}$
.8
.9
1.0
1.1
1.2
1.3
1.4
1.5
p_f fm^{-1}

Fig. 3

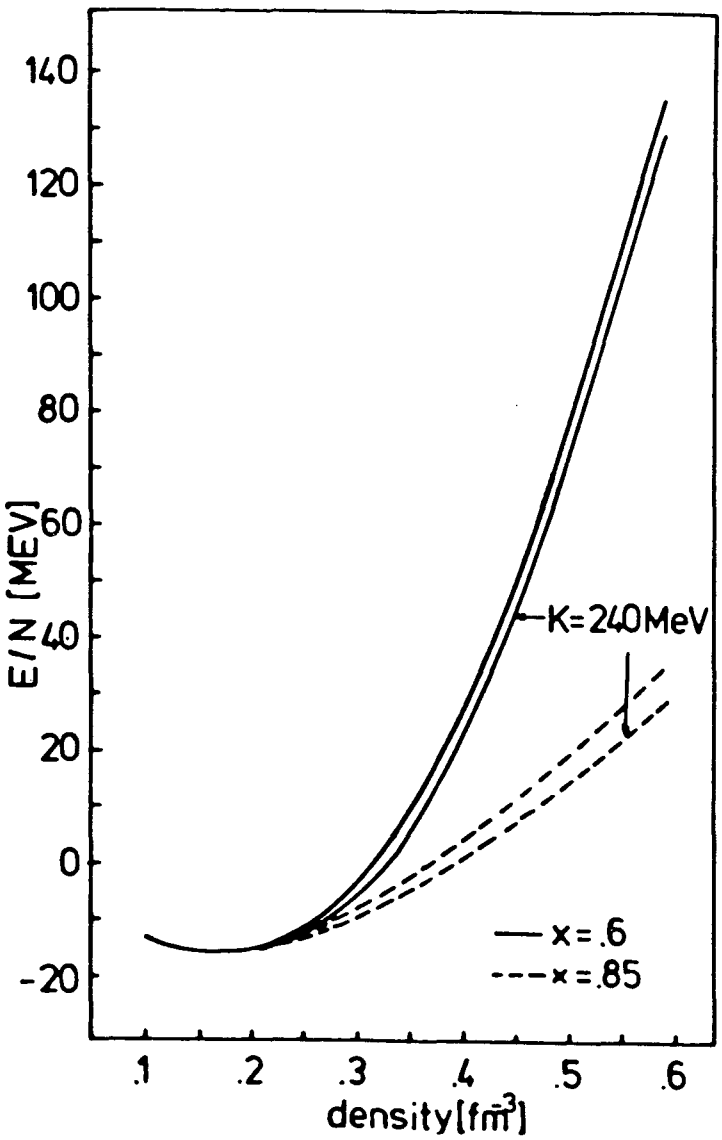
140
120
100
80
60
40
20
0
-20
E/N [MEV]
K=240MeV
x=.6
x=.85
.1
.2
.3
.4
.5
.6
density[fm^{-3}]

Fig. 4

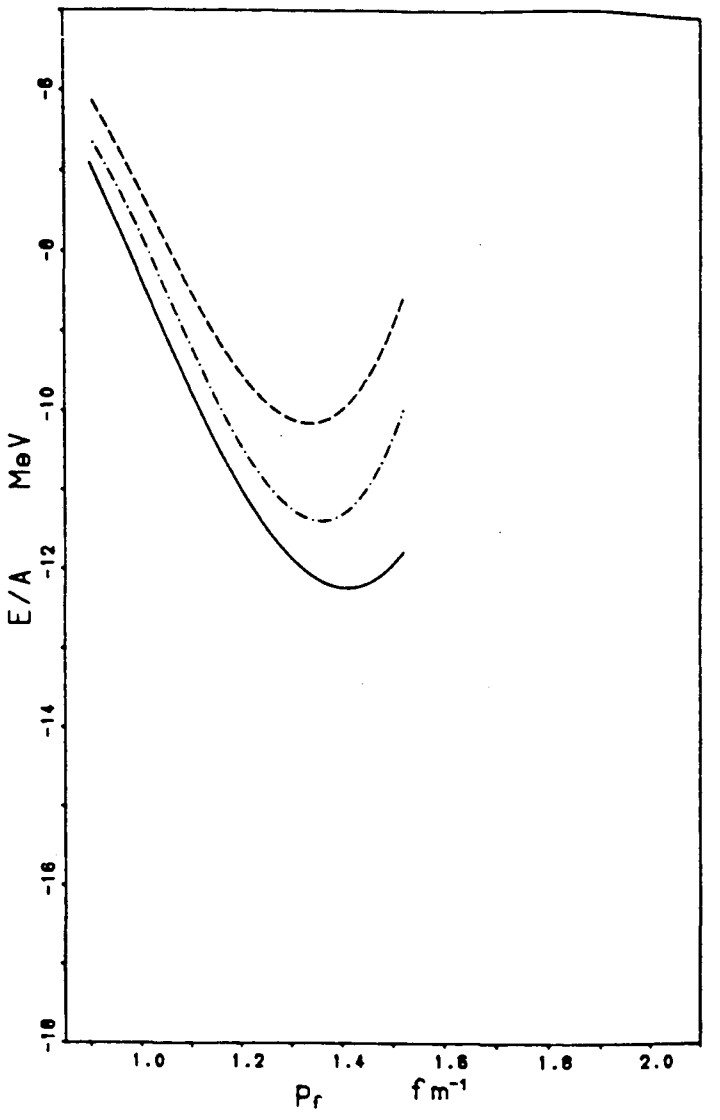
E/A MeV
-6
-8
-10
-12
-14
-16
-18
1.0
1.2
1.4
1.6
1.8
2.0
P_f fm^{-1}

Fig. 5

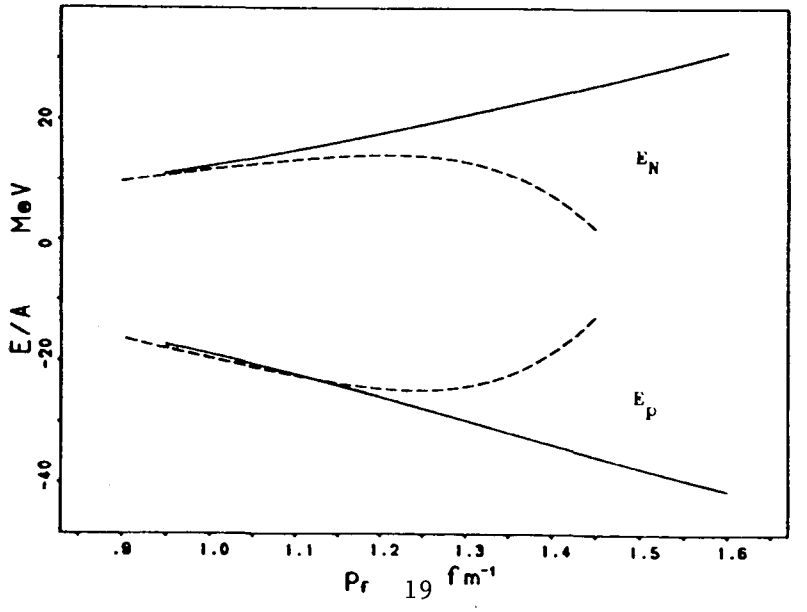
E/A MeV
20
0
-20
-40
E_N
E_p
.9
1.0
1.1
1.2
1.3
1.4
1.5
1.6
P_f fm^{-1}

Fig. 6

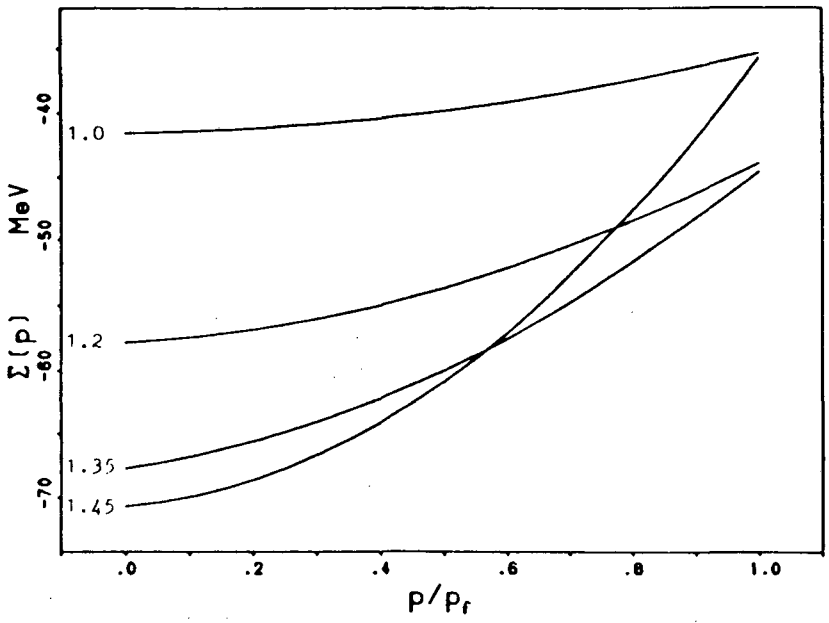
-40
-50
-60
-70
MeV
Σ(p)
1.0
1.2
1.35
1.45
.0
.2
.4
.6
.8
1.0
p/pf

Fig. 7

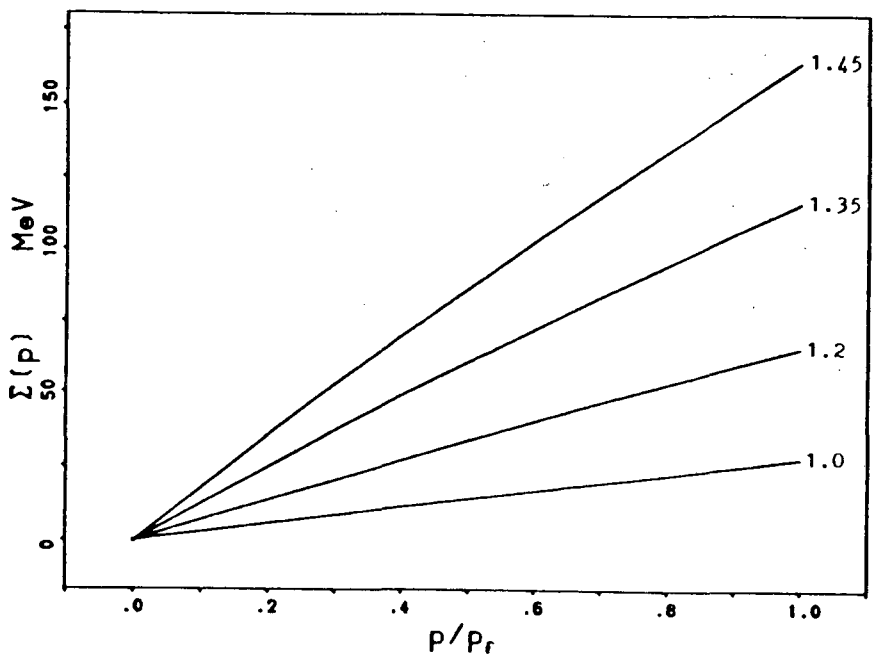
150
100
50
0
MeV
Σ(p)
1.45
1.35
1.2
1.0
.0
.2
.4
.6
.8
1.0
p/pf

Fig. 8

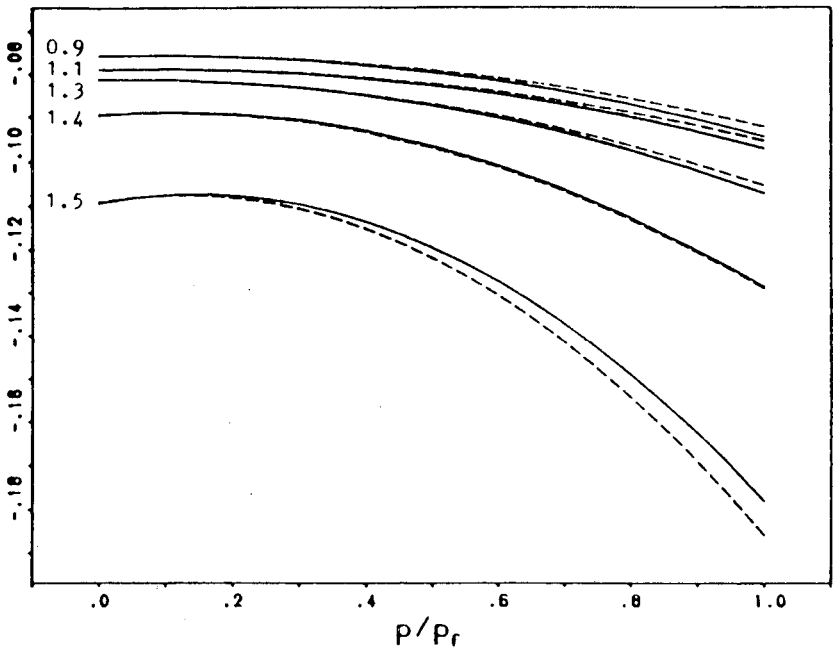
0.9
1.1
1.3
1.4
1.5
-.08
-.10
-.12
-.14
-.16
-.18
.0
.2
.4
.6
.8
1.0
p/pf

Fig. 9

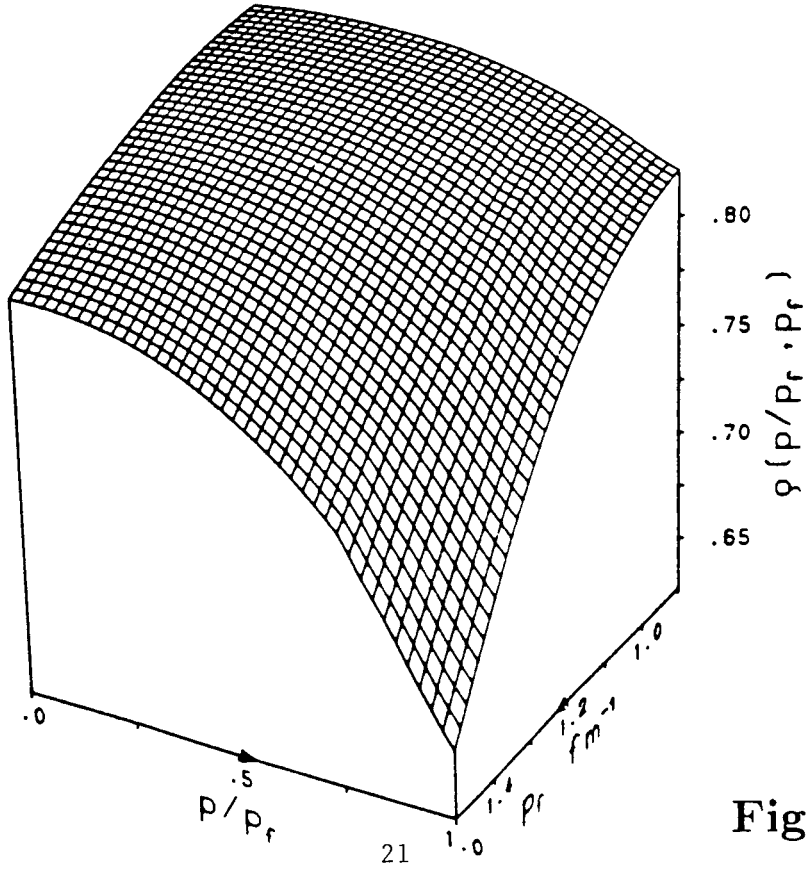
.80
.75
.70
.65
ρ(p/pf, pf)
.0
.5
p/pf
1.0
1.0
fm-1
pf

Fig. 10

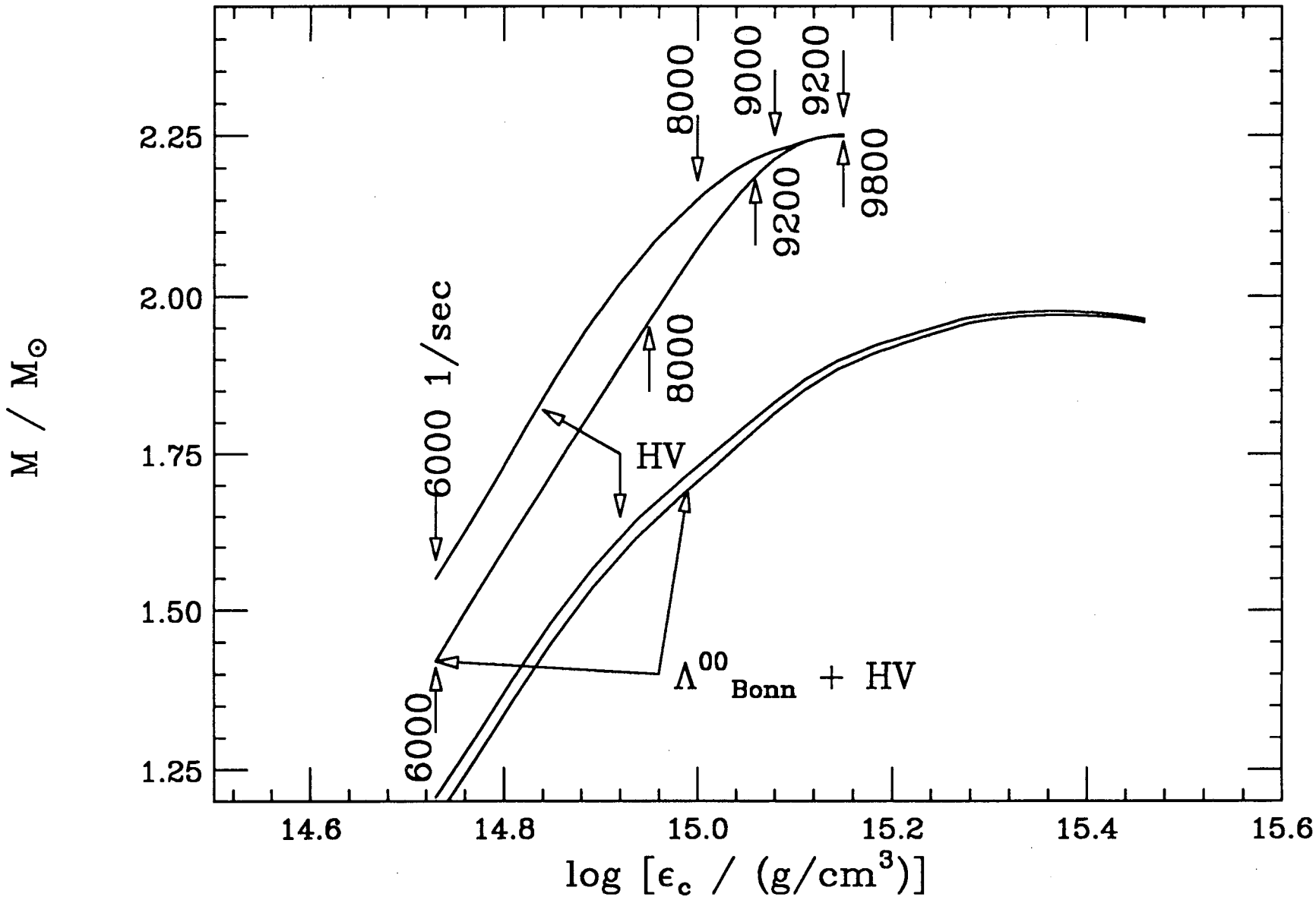
M / M⊙
2.25
2.00
1.75
1.50
1.25
14.6
14.8
15.0
15.2
15.4
15.6
log [ϵc / (g/cm3)]
8000
9000
9200
9800
9200
8000
6000 1/sec
HV
Λ00Bonn + HV
6000

Fig. 11

LAWRENCE BERKELEY LABORATORY
UNIVERSITY OF CALIFORNIA
INFORMATION RESOURCES DEPARTMENT
1 CYCLOTRON ROAD
BERKELEY, CALIFORNIA 94720